Computer Three-Dimensional Reconstruction of the Atrioventricular Conduction System

RAJA KANNAN MUTHARASAN, ASHWIN NAGARAJ, ANDREW J. HAMILTON, DAVID D. McPHERSON, and SAROJA BHARATI*

From the Northwestern University Medical School, Chicago, and the *Maurice Lev Congenital Heart and Conduction System Center, Advocate Hope Children's Hospital, Advocate Christ Medical Center, Oak Lawn and Rush-Presbyterian St. Luke's Medical Center, Chicago, Illinois

MUTHARASAN, R.K., ET AL.: Computer Three-Dimensional Reconstruction of the Atrioventricular Conduction System. *The human atrioventricular conduction system (AVCS), which includes the AV node and its approaches, AV bundle (penetrating, branching, and bifurcating parts), and the bundle branches, is a curved complex structure that has not been reconstructed in three dimensions using computer technology. Microscopic slides of every 40th serial section (cut at 7 micron level) of the AVCS were digitized into 600 dots/inch color images. External outlines of each section were manually segmented using commercially available three-dimensional rendering software (Rhinoceros). The AVCS was traced from light microscopy and superimposed onto the external outlines. To account for inherent errors in histological slide preparation, an optimization procedure was used to align external outlines of all sections. The optimal rotation and translation of each section was established by maximizing area of overlap between adjacent sections. A sequential one-dimensional minimization algorithm was used for optimization. Rotation and translation values were then used to align external outlines and the superimposed conduction system, reconstructing the AVCS in three-dimensions. To validate the method, the algorithm was applied to a digitized image transformed with known translations and rotations. The validation procedure demonstrated that each test image aligned in translations and to within 0.01 degree in rotations. Spatial error determined by resolution of the digitized images was ±0.5/600 inch (±21 microns). Three-dimensional reconstruction of every 40th serial section clearly demonstrated the complex curved shape of the AVCS. Three-dimensional reconstruction of the human and canine AVCS permits accurate pathological and electrophysiological correlation of the conduction system. (PACE 2004; 27[Pt. I]:740–748)*

atrioventricular conduction system, pathology, serial sections, computer-assisted three-dimensional reconstruction, optimization

Introduction

The human atrioventricular conduction system (AVCS) has not been accurately modeled by using computer technology in three dimensions directly from serially sectioned histological studies. The AVCS is a complex curved structure, and the lack of accurate models has limited clinical and pathological correlations.[1–3] One technical challenge in developing such models is the proper orientation of the serial sections in relation to one another in the absence of reference markers for alignment. The second challenge is the creation of models detailed enough to reveal the microscopic variations seen in the AVCS.[1–3] Another difficulty is the rapid and simple visualization of such models from all angles once constructed. The advent of powerful desktop computers capable of performing computationally intense alignment algorithms in reasonable time frames and rendering, moving, and displaying detailed three-dimensional models in real time may now provide a means to accurately display the AVCS.

Braverman and Braverman[4] demonstrated the feasibility of using a microcomputer graphics system to generate a three-dimensional reconstruction of a hemangioma from serial sections. Further work using computer-assisted three-dimensional reconstruction of serial sections by other groups has demonstrated the three-dimensional structure of the rabbit hippocampus[5] and that of osteons in cortical bone.[6] In an effort to minimize alignment errors in these reconstructions, some groups have used external markers prior to sectioning[7,8] and computer and image analysis methods[9,10] with varying degrees of success. In the cardiovascular system, three-dimensional reconstruction efforts have mostly been restricted to three-dimensional visualizations of the heart and great vessels.[11]

Presented in part at the American College of Cardiology Scientific Sessions, Orlando, FL, March 2001.

Supported in part by the Feinberg Cardiovascular Research Institute.

Address for reprints: Saroja Bharati, M.D., Maurice Lev Congenital Heart and Conduction System Center, 11745 Southwest Highway, Palos Heights IL 60463. Fax: (708) 361-8673; e-mail: bharati@thic.com

Received July 22, 2003; revised January 5, 2004; accepted February 5, 2004.

This article demonstrates a method of accurately reconstructing and displaying a three-dimensional model of the specialized AVCS in the human and the canine by using modern computer technology.

Materials and Methods

Materials

The materials used were the:

- Adobe Photoshop 5.5 imaging software (Adobe Systems Inc., Palo Alto, CA, USA)
- Desktop scanner (Microtek, Redondo Beach, CA, USA)
- Histological slides of the AVCS
- Light microscope (Nikon Corp., Melville, NY, USA)
- Pentium II desktop computer (Dell Computer Corp., Round Rock, TX, USA)
- MATLAB 5.1 mathematical software (The Mathworks, Inc., Natick MA)
- Microscope video camera (Javelin Electronics, Japan)
- Rhinoceros 1.1 three-dimensional modeling software (Robert McNeel & Associates, Seattle, WA, USA)
- Sony Trinitron monitor - PVM-14M4U (Sony Corp., Japan)

Methods

The method of study of the conduction system pathologically has been previously published.[1–3]

Briefly, blocks were taken from the sinoatrial (SA) node and its approaches, the atrial preferential pathways, the atrioventricular (AV) node and its approaches, the AV bundle (penetrating, branching, and bifurcating parts), and the bundle branches up to the region of the moderator band, and serially sectioned. Every 20th section is retained and alternate sections are stained with hematoxylin-eosin and Weigert-van Geison stain. In addition, several sections are taken from the remainder of the heart. Depending on the size of the heart, approximately 1,200–1,600 sections were obtained for the study of the entire conduction system in an adult. The sections were then compared with those from an age-matched control conduction system. This method of sectioning and sampling the entire heart yields a semiquantitative analysis of the conduction system.

Cases

The AVCS was reconstructed from four separate sets of slides from four different hearts. For the study of the AVCS, the parietal walls of the right and left atria and ventricles are separated from the atria and ventricles. To fashion the blocks containing the approaches to the AV node, the AV node bundle, and bundle branches, a cut is made along a line just posterior to the moderator band and the right anterolateral papillary muscle at an angle of almost 45 degrees to the septal band of the crista supraventricularis and passes below the crux of the heart. A second cut is made in the upper aspect of the atrial septum from the roof of the aorta to the center of the fossa ovalis. The third cut is made at right angles to the first cut along a line proximal to the insertion of the eustachian valve so that the coronary sinus region is in the block and the crux. A fourth cut is made through the lower part of the arch of the crista parallel to the baseline, making sure that the base of the aorta and most of the pars membranacea are in the block.[1–3]

These blocks that contain the AV node, AV node bundle, and bundle branches are then subdivided into portions depending on the pathology expected. Usually it is subdivided by cuts through the pars membranacea, proximal to the insertion of the tricuspid valve, and through the muscle of Lancisi. Further cuts are made up to the moderator band.

These blocks containing the AV node, AV node bundle, and bundle branches are now sent through the Peterfi double embedding method.[1–3]

The slides were then prepared by cutting tissue blocks containing the AVCS into serial sections of 7 μm thickness, retaining every fifth (Q5) or twentieth (Q20) section, and staining each retained section alternately with hematoxylin-eosin or Weigert-van Gieson stains. This provided the data sets at Q10 or Q40 for reconstruction. The four data sets used for reconstruction were:

1. A 16-year-old female human, the block containing the AVCS, including the approaches to the AV node, AV node, penetrating and branching AV bundle, and the beginning of the left and right bundle branches, a total of 45 sections at Q40.
2. A 1-month-old male human, the block containing the AVCS from the approaches to the AV node to the bifurcation of the bundle of His, a total of 50 sections at Q10. This case was sectioned at Q5 to determine if closer sectioning would improve the accuracy of the three-dimensional reconstruction.
3. An adult male canine, the block containing the AVCS from the approaches to the AV node to the left and right bundle branches, a total of 50 sections at Q40.
4. An adult male canine, the block containing the SA (SA) and AV nodes, up to the region of the AV bundle with an ablation of the SA node and the surrounding atria, a total of 50 sections at Q40.

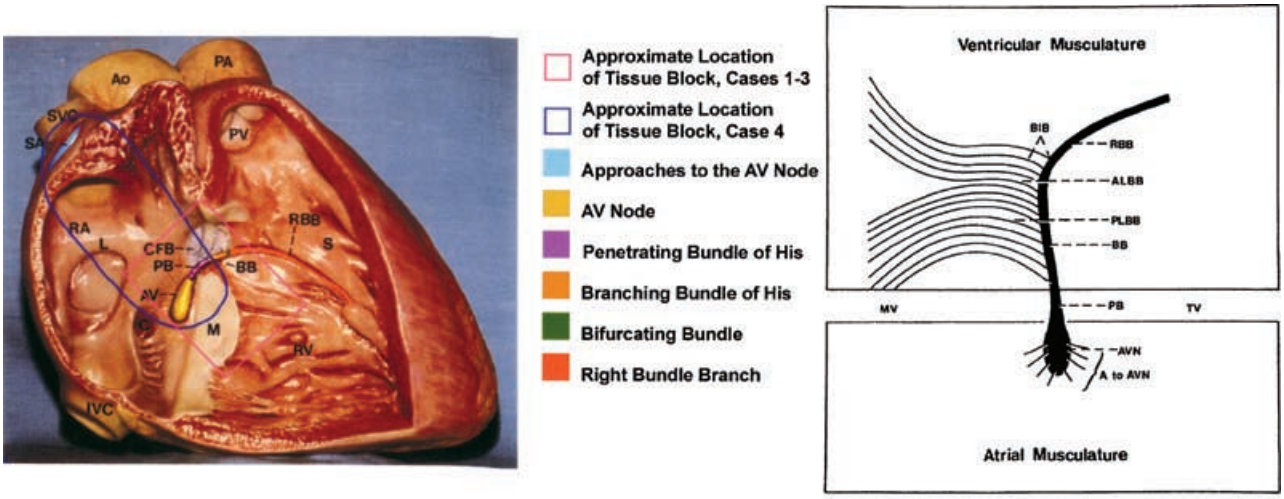

Figure 1. *A heart model (left) demonstrating the tissue block taken for the study of the serial sections, and a schematic diagram (right) of the normal atrioventricular conduction system. AV = atriovenricular; AVN = atrioventricular node; A to AVN = approaches to the AV node; PB = penetrating AV bundle; BB = branching AV bundle; BIB = bifurcating AV bundle; PLBB = posterior radiation of left bundle branch; ALBB = anterior radiation of left bundle branch; RBB = right bundle branch; TV = tricuspid valve; MV = mitral valve; RA = right atrium; RV = right ventricle; PV = pulmonary valve; Ao = aorta; PA = pulmonary artery; S = septal band; M = medial leaflet of the tricuspid valve; CFB = central fibrous body; L = limbus; SVC = superior vena cava; SA = sinoatrial node; IVC = inferior vena cava.*

Figure 1 shows a heart model demonstrating the location of the tissue block for the above cases, and a schematic diagram of the normal conduction system for comparison with the three-dimensional reconstructions. Since the human and canine AVCS are similar but not identical, the above four hearts were chosen to compare the feasibility of three-dimensional reconstruction in both situations.

Digitization of Slides and Manual Segmentation

The sections stained with Weigert-van Gieson stain constituted the set of slides used for reconstruction of the AVCS. These slides were digitized using a standard document scanner. Each digital image corresponded to one histological section and was acquired at a resolution of 600 dots/inch (dpi) in 24-bit red-green-blue (RGB) color, and saved in JPEG format using maximum quality settings (Fig. 2). Each image was 600 pixels in width and 1,100 pixels in height.

The digital images were loaded successively as background templates into Rhinoceros, a commercially available three-dimensional imaging/rendering software. The digital images of $600 \times 1{,}100$ pixels were loaded as an image in Rhinoceros of 60×110 length units. Since 600 pixels (60 Rhinoceros length units) corresponded to 1 inch, one Rhinoceros length unit corresponded to 423 μm and is 10 pixels. The images were loaded in the XY plane containing the origin and were centered on the origin. All the images were loaded in this same position. The external outline of each section was manually traced as a closed curve so that the outline of each section could be manipulated and eventually visualized when rendering the model (Fig. 3). The parts of the AVCS lying in each section were also manually traced as closed curves (Fig. 3). This was accomplished by comparing the background-loaded template to the appearance of the corresponding histological section. This was performed at X40 magnification under light microscopy viewed on a monitor, and then identifying the pixels in the digitized image corresponding to structures of the AVCS. A closed curve was then manually traced around these pixels. The closed curves representing the AVCS and the outline of the gross tissue block from each section were then assigned the same unique layer, creating a "virtual slide" (Fig. 2). Each virtual slide could then be moved en bloc in relation to one another.

After the outlines of the AVCS and the gross tissue block from one slide were saved to the same layer, the background image was removed, and the slide was moved in the z-dimension to its correct place in the reconstruction. The first step in this procedure was to calculate the appropriate spacing distance. In cases 1, 3, and 4, every 40^{th} section was mounted onto a slide, stained with Weigert-van Gieson stain, and used in the reconstruction. Since each slide was cut to a 7-μm thickness, the spacing distance of these slide sets was 280 μm

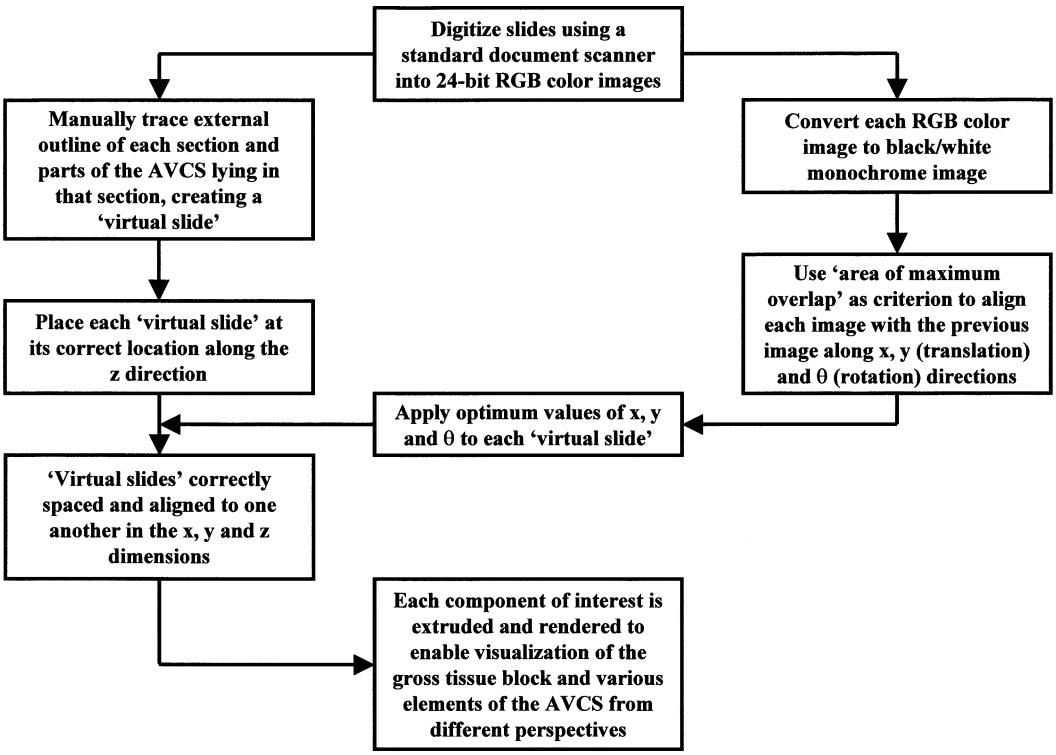

Figure 2. *Schematic diagram showing the steps involved in digitization of slides, manual segmentation, translational and rotational alignment, and final rendering of the gross tissue block and the atrioventricular conduction system (AVCS).*

or 0.661 Rhinoceros length units. In case 2, every tenth slide was used, which resulted in a spacing distance of 70 μm or 0.17 Rhinoceros length units. The slide was positioned below the slide preceding it by the appropriate spacing distance, and the background image corresponding to the next slide was loaded. This tracing and moving procedure was repeated until all the slides in a set were positioned.

At this point, the Rhinoceros files consisted of virtual slides correctly spaced in the z-dimension (vertically), but not correctly rotated or translated (horizontally) relative to one another. To determine the correct distances and angles through which the virtual slides had to be translated and rotated, an optimization algorithm was written in MATLAB, a commercially available mathematical software.

Translational and Rotational Alignment

The first step in the optimization procedure was to convert each of the color images associated with each section into a black and white monochrome image to simplify the procedure (Fig. 2). A program was written to evaluate the average color value of the red, green, and blue channels of each pixel in a JPEG image file, and create a new monochrome TIFF image file based on the color information. The average value of each pixel in the color JPEG image varies between 0 (black) and 255 (white). A threshold value of 200 was selected since it was the value that best differentiated the tissue section from the background in the JPEG file of the slide. If the average color value of a pixel was >200 the pixel was assigned the value 0, and if it was 200 it was assigned the value 1 in the new TIFF file. The TIFF files generated by the program were then manually edited to remove any pixels that represented background artifacts. At this stage the TIFF files represented the tissue section in white pixels and the background in black pixels. The monochrome TIFF files were then used as the basis for the optimization procedure.

The monochrome image corresponding to the first section was taken as the base image, to which all other sections would ultimately be aligned. The image corresponding to the second section was moved by the program in the translational (x, y) and rotational (θ) directions. This step was performed until the white area of the second section, corresponding to the tissue block, maximally overlapped with the white area of the first section. The values leading to an optimum translation and rotation were stored. The third section was aligned with the optimally translated and rotated second

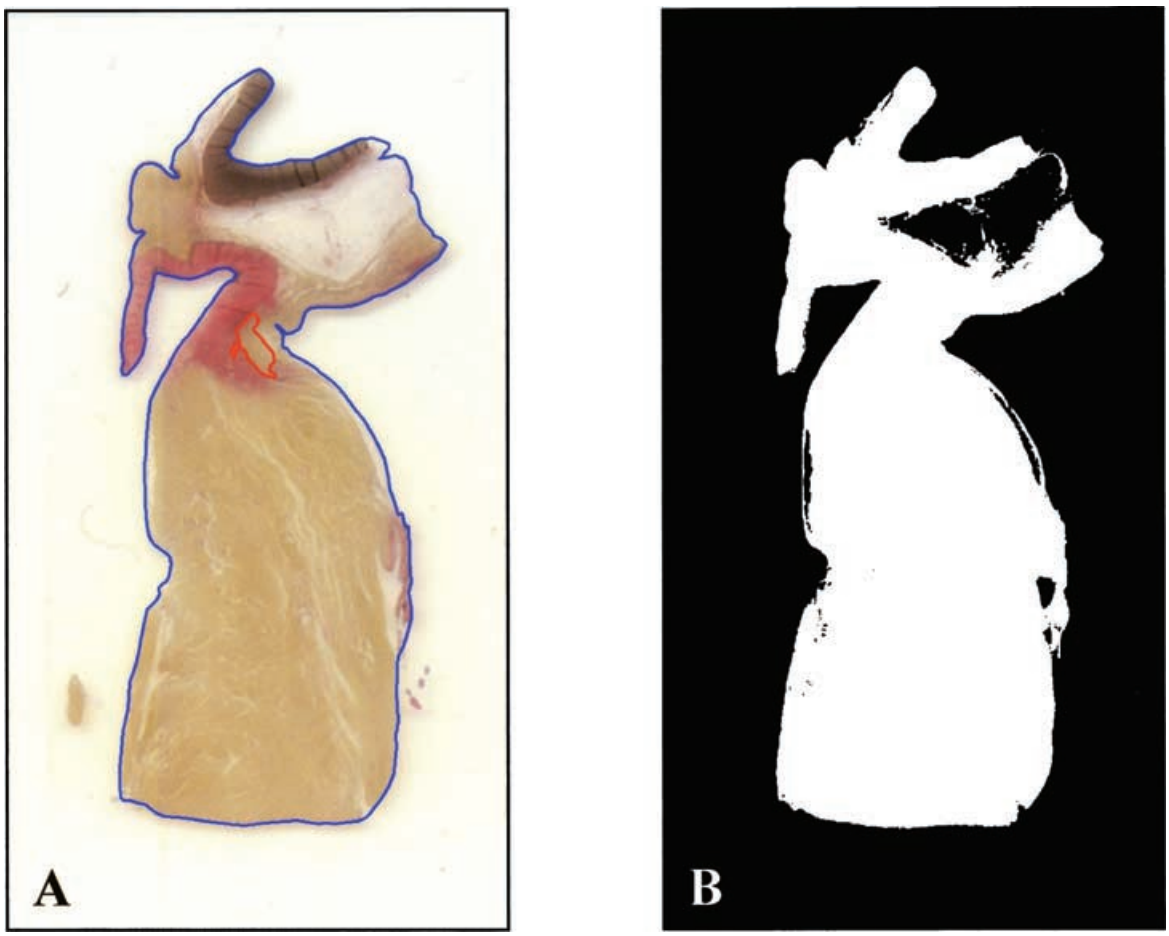

Figure 3. *(A) A representative red-green-blue (RGB) color image of a digitized slide showing the tissue section and the manually segmented external outline (blue) and parts of the atrioventricular conduction system lying in that section (red). (B) The same color image converted to a black and white monochrome image, with white areas representing the tissue section and the background in black. This monochrome image is used in the translational and rotational alignment procedure.*

section, and the optimum translation and rotation values stored. This procedure was repeated until all the sections from the tissue block were aligned to the slide preceding it (Fig. 2).

The misalignment between two consecutive sections is defined as the cost function for the optimization procedure. For any slide n and the subsequent slide n + 1, the program optimized the area of overlap of the tissue blocks by minimizing the cost function defined as the absolute value of the difference between the matrix representing slide n and the matrix representing slide n + 1 rotated through θ degree and translated by X pixels in the x-direction and Y pixels in the y-direction. This was accomplished by using an iterative sequential one-dimensional optimization method. The optimum value for θ was first found using a golden section search method,[12] to an accuracy of 0.01 degree. The optimum values for Y and X were then found using an equal interval search method.[12] This constituted the first iteration of the optimization procedure. Iterations were continued in the order of θ, Y, X. The iterations were halted when there was no change in the values of θ, Y, X from the iteration before. The optimization procedure was then repeated until the entire slide set was aligned.

The transformations derived in MATLAB for each slide were then applied to each virtual slide in the Rhinoceros file (Fig. 2). At this point the file contained virtual slides correctly spaced and aligned to one another in the x, y, and z dimensions. Each element on the virtual slide was then extruded into a solid and given a color and transparency so that the gross tissue block and the various elements of the AVCS could be visualized (Fig. 2). The completed three-dimensional AVCS

models were then viewed from various angles, and screen captures were taken to provide two-dimensional images of the models.

Validation of Optimization Procedure

The optimization procedure was validated by selecting an arbitrary TIFF file representing a slide, rotating and translating it by known amounts, and saving to a second TIFF file. The two images were then fed into the alignment routine. The stability of the optimum solution with changes in the starting point and the effect of one-dimensional search order was also determined.

Results

The validation procedure demonstrated that the optimization algorithm aligned the test images precisely, resulting in a cost function value of zero. Hence, the optimization procedure aligned the slides extremely well in translations and to within 0.01-degree in rotations. Also, the optimization algorithm used was robust, converging to the optimum from starting points up to ± 100 pixels (x, y) and ±30 degrees (θ) away. It was also found during the validation process that the cost function value is most sensitive to changes in θ and the fastest convergence times are seen when the rotation θ is minimized first, and then the translations x and y.

On average, it took approximately 10 minutes for the optimization algorithm to align a slide with the previous one. Hence, for a slide set with 50 serial sections, the computation time was approximately 8 hours.

Figures 4-7 illustrate the aligned three-dimensional reconstructions of the AVCS for cases 1–4, respectively. The figures show the reconstructed AVCS from two different viewpoints and demonstrate its complex curved shape. Figures 4 and 5 demonstrate the AV node and its approaches, the AV bundle (penetrating, branching and bifurcating portions), and the beginning of the left and right bundle branches in the human specimens. Figure 5 (case 2, slide retention at Q10) demonstrates a reconstruction with greater resolution as compared with the reconstructions in Figure 4 (case 1, slide retention at Q40). It is to be pointed out that in both cases, the AVCS is a curved structure, though not identical from case to case.

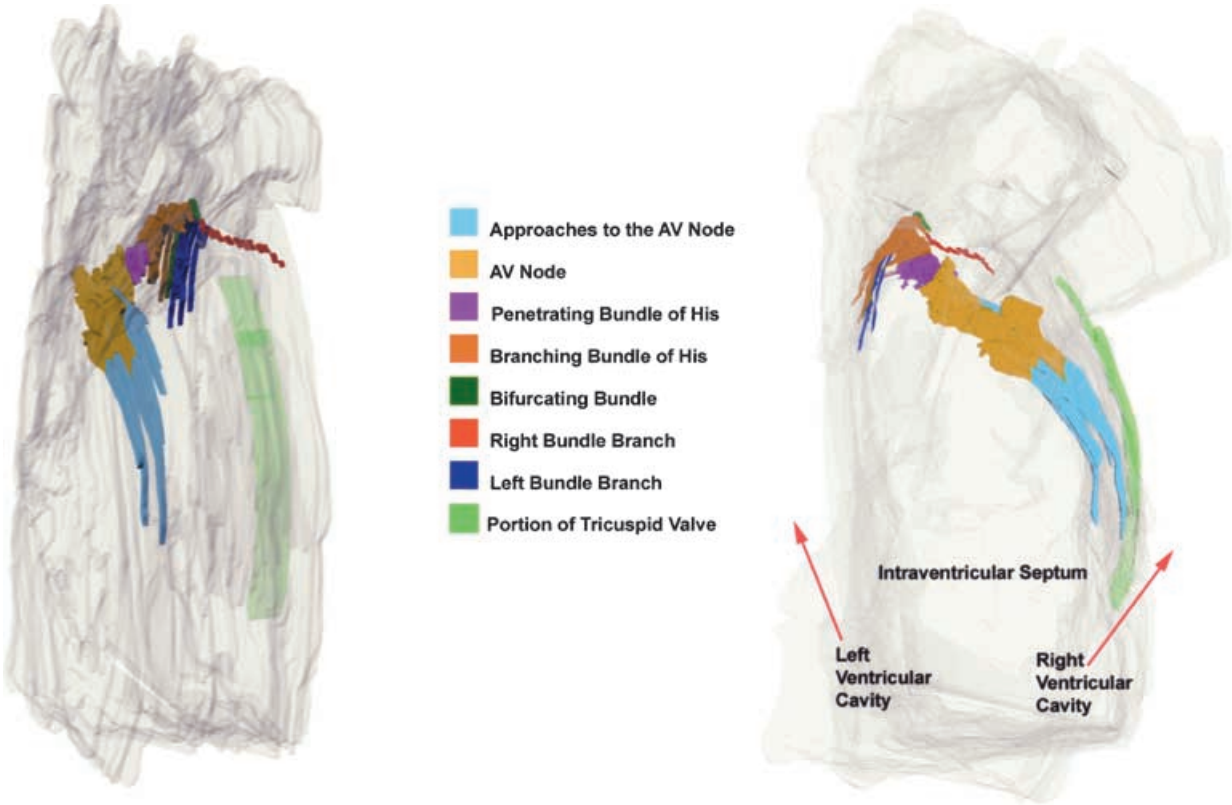

Figure 4. *Three-dimensional reconstructions of case 1 showing the view from the right ventricle (left) and from the proximal to distal atrioventricular conduction system (right).*

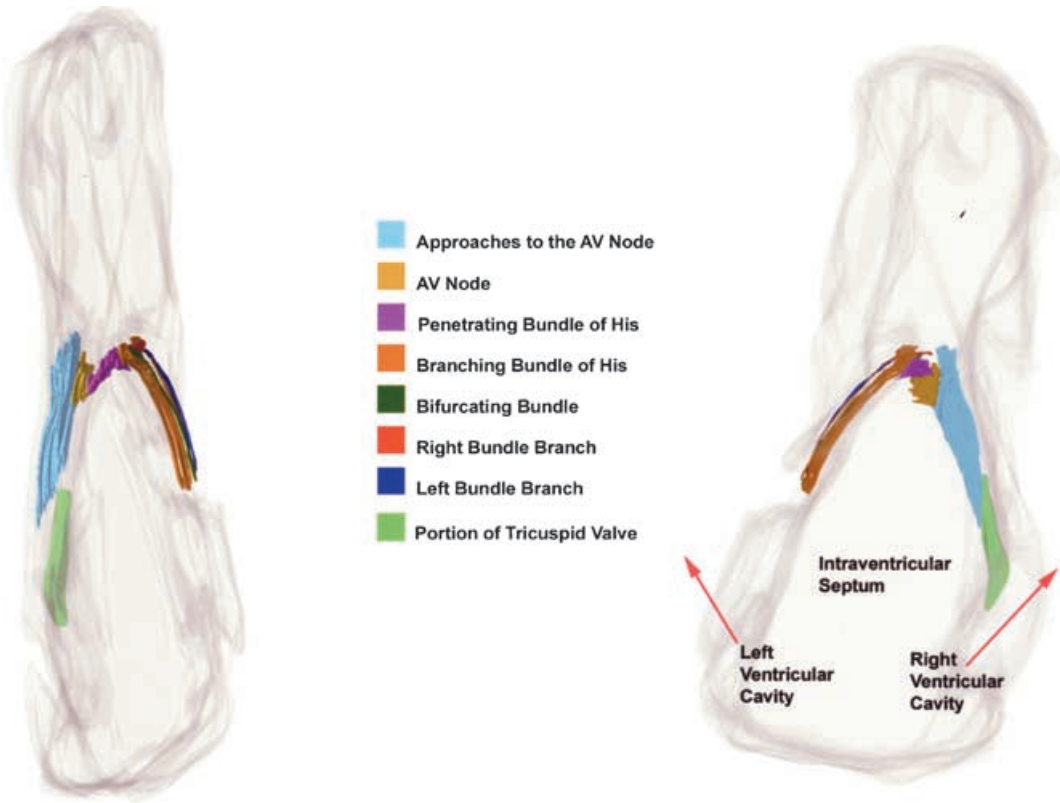

Figure 5. *Three-dimensional reconstructions of case 2 showing the view from the right ventricle (left) and from the proximal to distal atrioventricular conduction system (right).*

Figure 6 (case 3, slide retention at Q40) demonstrates the AV node and its approaches, the AV bundle (penetrating, branching, and bifurcating portions) and the beginning of the left and right bundle branches in a canine specimen. Figure 7 (case 4, slide retention at Q40), also from a canine specimen, shows a tissue block taken from the SA node to the AV nodal junction in a circular fashion. This reconstruction demonstrates the SA node, the AV node, the ablated area between the two nodes and the penetrating AV bundle. Despite the difference in the tissue block in cases 3 and 4, the three-dimensional reconstructions clearly demonstrate that the AVCS in the canine is also curved and complex, similar to the human AVCS.

Discussion

Our discussion will focus on the implications and limitations of our results. We have described a computer method for the alignment and 3D reconstruction of the human and canine atrioventricular conduction system from histological serial sections. The method accurately reconstructed the AVCS in both species. Also, given the size of the conduction system, slide retention at Q40 appeared to be sufficient for accurate reconstruction as compared with Q10 retention.

The alignment algorithm presented is robust. Spatial errors due to the alignment procedure could potentially arise only from the rotational precision of 0.01 degree. This error is negligible since for an image size of 600×1100, a rotation <0.01 degree will not cause any pixel to change position. Hence, spatial errors are only due to the digitization process (quantization error) and are of the order of ± 0.5 pixel, which corresponds to an error of about ± 21 μm.

The method described is a simple and relatively efficient method that correctly aligned the slides according to their maximum overlap. The cost function for the slide sets to be aligned was smooth and well behaved and had only one minimum value, the point of maximum alignment. There were no local minima in the cost function. This allowed the use of a relatively simple alignment strategy. Since there were no local minima, for any given variable the value of the cost function would always decrease when moving towards greater alignment and increase when moving towards less alignment. As the cost function had only one minimum value, it was possible to use a simple iterative search sequence consisting of a set of sequential one-dimensional minimizations.

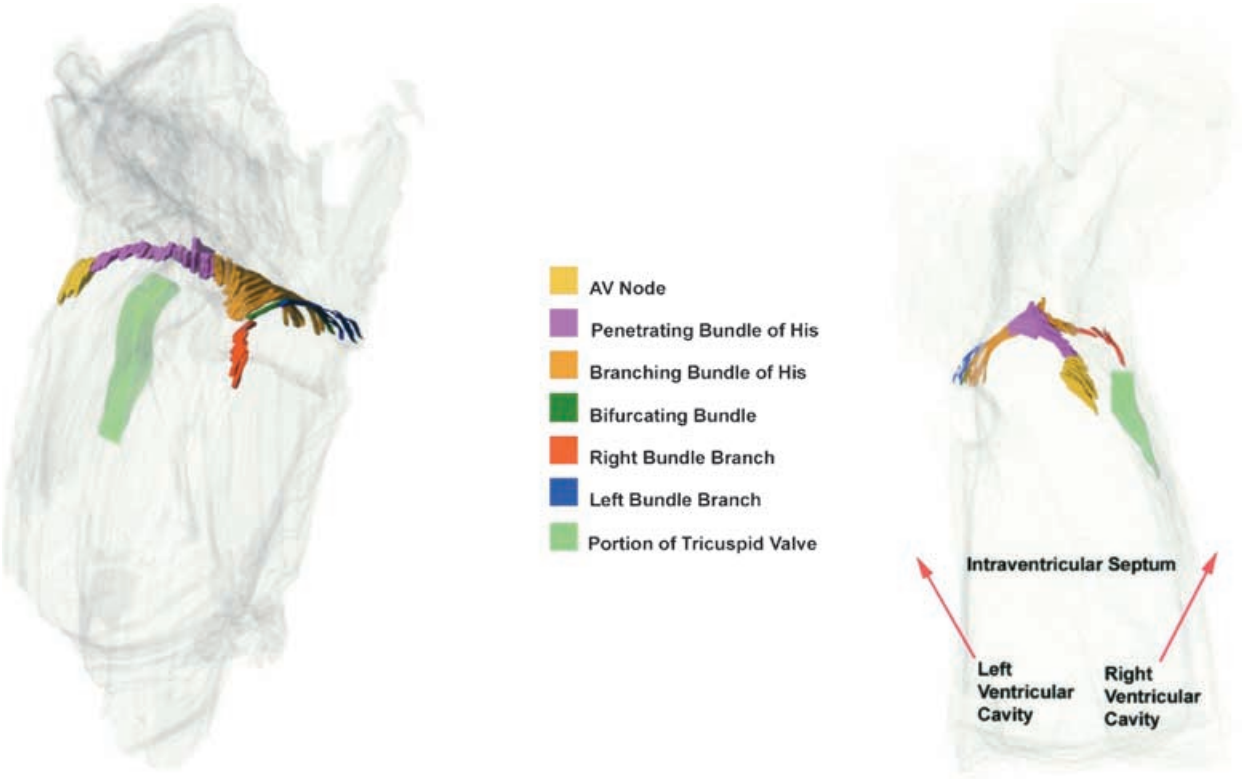

Figure 6. *Three-dimensional reconstructions of case 3 showing the view from the right ventricle (left) and from the proximal to distal atrioventricular conduction system (right).*

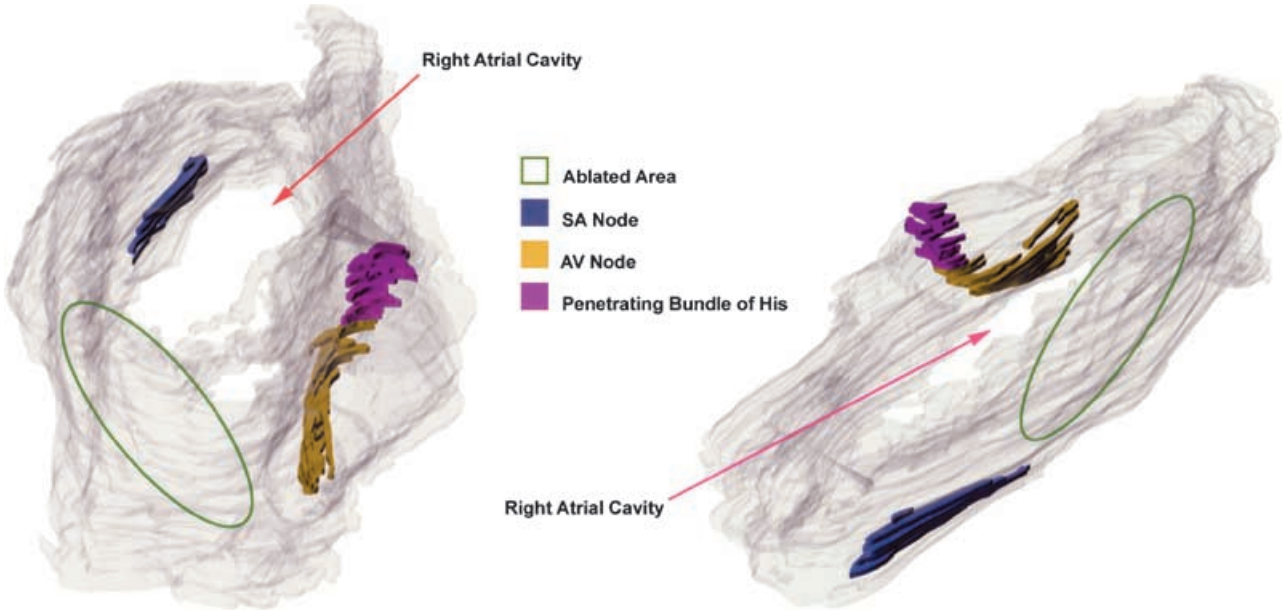

Figure 7. *Three-dimensional reconstructions of case 4 showing the view from the right ventricular (left) and from the sinoatrial node (right).*

Study Limitations

There were some limitations to the study. The area of maximum overlap used in the optimization strategy may not necessarily correspond to the true orientation of the tissue sections. The true structure may be skewed minimally to one side or the other. The authors believe that this distortion is minimal because sections containing anatomic landmarks, like the posterior leaflet of the mitral valve, which typically measured roughly 30 pixels (1.2 mm) in width, aligned well in the reconstructed model. Previous studies[7,8] have used tissue block markers prior to microtoming to align tissue sections. Due to the distortion produced by microtoming, these methods required complex transformational algorithms to realign tissue markers. The authors have, therefore, developed a method of alignment that does not rely on tissue markers but directly on the tissue section itself.

A second limitation of the study is the histological procedure (including the Peterfi method) itself, which introduces two types of error: shrinkage during fixation, dehydration, and infiltration and expansion during sectioning, floating-out, and mounting. The overall microtomy induced section distortion is the sum of the above two errors. Jones et al.[13] measured distortion errors induced while preparing different types of rat tissues and found them to be 1% for liver, 8% for kidney, 7% for lung, and 20% for skeletal muscle. Similar work by others on dog and sheep hearts found that overall distortion errors during cardiac tissue processing were in the order of 5%.[14] By applying the above distortion error to our data, the maximum possible distortion in the y-direction is about 50 pixels (~2 mm) and in the x-direction 25 pixels (~1 mm). The direct tissue alignment method that presented in this study is specifically designed to minimize this distortion error.

Lastly, this method of reconstructing the AVCS is a labor-intensive process most limited in terms of speed by the tracing of the conduction system and the entire surrounding myocardium in the tissue block in Rhinoceros. However, with improved automation, this three-dimensional reconstruction methodology of the AVCS could be available to any cardiovascular pathology laboratory.

Significance of Study of the Conduction System by the Authors' Method

This computer method demonstrates that the AVCS is a curved complex structure and can be reconstructed in three dimensions. The utility of such methodology lies in its ability to allow better visualization of the cardiac conduction system. The conduction system forms a curve or an arch and is not in a straight line. Analysis of the conduction system for correlative studies with electrocardiographical and electrophysiological studies can only be obtained if blocks were taken in such a manner that the entire conduction system can be followed from the beginning to the periphery and these data constructed in three dimensions. An example is, in the study of sudden death in preexcitation, the task is to correctly find the bypass pathways. The three-dimensional method allows complete study of the AV rims and the conduction system. This knowledge may improve the techniques associated with interventional procedures like ablation of arrhythmic foci, pacing, and electrophysiological mapping.[15,16]

Acknowledgments: The authors thank A. Teti for manuscript preparation.

References

1. Lev M, Bharati S. A method of study of the pathology of the conduction system for electrocardiographic and His bundle electrogram correlations. Anat Rec 1981; 201:43–49.
2. Bharati S, Lev M. Sudden death in athletes- conduction system: Practical approach to dissection and pertinent pathology. Cardiovasc Pathol 1994; 3:117–127.
3. Bharati S, Lev M. The Cardiac Conduction System in Unexplained Sudden Death. Mount Kisco, NY, Futura Publishing Co., 1990,pp. 5–16.
4. Braverman MS, Braverman IM. Three-dimensional reconstructions of objects from serial sections using a microcomputer graphics system. J Invest Dermatol 1986; 86:290–294.
5. Andreasen A, Drewes AM, Assentoft JE, et al. Computer-assisted three-dimensional reconstruction of the hippocampal region based on serial sections. J Neurosci Methods 1991; 37:151–160.
6. Stout SD, Brunsden BS, Hildebolt CF, et al. Computer-assisted 3D reconstruction of serial sections of cortical bone to determine the 3D structure of osteons. Calcif Tissue Int 1999; 65:280–284.
7. Brandle K. A new method for aligning histological serial sections for three-dimensional reconstruction. Comput Biomed Res 1989; 22:52–62.
8. Streicher J, Weninger WJ, Muller GB. External marker-based automatic congruencing: A new method of 3D reconstruction from serial sections. Anat Rec 1997; 248:583–602.
9. Hibbard LS, Arnicar-Sulze TL, Dovey-Hartman BJ, et al. Computed alignment of dissimilar images for three-dimensional reconstructions. J Neurosci Methods 1992; 41:133–152.
10. Rydmark M, Jansson T, Berthold CH, et al. Computer-assisted realignment of light micrograph images from consecutive section series of cat cerebral cortex. J Microsc 1992; 165:29–47.
11. Chatel D, Martin-Bouyer Y, Acar C, et al. Three-dimensional modeling of the anatomy of the heart and great vessles. Surg Radiol Anat 1993; 15:341–348.
12. Arora JS. Introduction To Optimum Design. New York, NY, MacGraw Hill, 1989, pp. 287–304.
13. Jones AS, Milthorpe BK, Howlett CR. Measurement of microtomy-induced section distortion and its correction for 3-dimensional histological reconstructions. Cytometry 1994; 15:95–105.
14. McLean M, Prothero JW. Three-dimensional reconstruction from serial sections. V. Calibration of dimensional changes incurred during tissue preparation and data processing. Anal Quant Cytol Histol 1991; 13:269–278.
15. Bharati S, Lev M. The morphology of the AV junction and its significance in catheter ablation. (editorial) PACE 1989; 12:879–882.
16. Bharati S, Lev M. Sequelae of atriotomy and ventriculotomy of the endocarium, conduction system and coronary arteries. Am J Cardiol 1982; 50:580–587.